STRUCTURE AND CHARACTERISTICS OF DETACHED TURBULENT FLOW IN A CAVITY

I. M. Varfolomeev, G. A. Glebov,
Yu. F. Gortyshov, A. N. Shchelkov,
and R. A. Yaushev

UDC 532.517.4+536.24

The results of an experimental investigation of the turbulence characteristics of detached flow in a channel with a rectangular cavity are given.

Detached turbulent flow which develops as a result of a gas or liquid flowing around a two-dimensional cavity has attracted the attention of many researchers, most of whom are presently endeavoring to devise a reliable calculation method based on a certain turbulence model [1, 2]. As has been noted in several papers, adoption of an acceptable turbulence model which would also have the highest degree of universality is complicated by the fact that the turbulence characteristics of flow in a cavity have not yet been sufficiently investigated. The aim of this article is to fill this gap to some extent. It should be noted that investigation of turbulent flow in cavities by means of the usual hot-wire anemometer methods is difficult, since a hot-wire anemometer produces considerable measurement errors in regions with intensive turbulent fluctuations and a low mean velocity (near the vortex center and the points of flow separation and attachment). These errors are connected with the lack of sensitivity of hot-wire anemometers to 180° direction reversals of the instantaneous velocity vector that occur in these flow regions. Therefore, most attention in this paper is focused on flow in the mixing layer above the cavity and also in the boundary layer at the cavity bottom, where the instantaneous velocity vector does not reverse its direction.

The experimental investigation was performed in a subsonic wind tunnel operating on the suction principle. The tunnel comprises the following basic parts: a profiled air intake with a filtering screen at the inlet, a test section, a honeycomb, and a centrifugal fan. The test section consists of a flat channel with a length of 3000 mm, a width of 380 mm, and a height of 140 mm. A rectangular cavity with a width of 380 mm was attached by butt-joining to the wider wall. The cavity length L was constant in the experiments (150 mm), while the depth H varied (75 and 150 mm), which corresponded to relative depth values H/L = 0.5 and 1.0.

The flow velocity in the channel was equal to $u_0 \sim 29$ m/sec, while the degree of turbulence was $\sqrt{\overline{u_0'^2}}/u_0 \approx 0{,}009$. The Reynolds number, calculated with respect to the cavity length, was equal to $\mathrm{Re}_L = u_0 L/\nu \approx 2{,}9 \cdot 10^5$. A well-developed turbulent boundary layer with the thickness $\delta/H \approx 0{,}08$ formed ahead of the separation point.

The mean velcoity u, the rms values of turbulent velocity fluctuations $\sqrt{\overline{u'^2}}$, and the energy spectra of velocity fluctuations were measured in the experiments. On the basis of Taylor's hypothesis concerning turbulence transfer by the averaged motion [3], the measured spectra were used for determining the longitudinal integral turbulence scales $l_u = \frac{\pi}{2} \lim_{k \to 0} F(k)$, where F(k) is the normalized wave number spectrum, $k = \frac{2\pi}{u} f$ is the wave number, and f is the frequency (Hz). The friction stress at the cavity bottom was found directly with respect to the slope of the averaged velocity profile in the viscous sublayer $\tau = \mu \partial u/\partial y$.

The measurements were performed by means of a DISA-55M hot-wire anemometer set, including a 55M01 constant-temperature hot-wire anemometer, a 55M25 linearizer, and a 55D31 digital mean-value integrating voltmeter. The rms values of velocity fluctuations were recorded by means of a V3-57 voltmeter. The energy spectrum of turbulence in the frequency range 1.5-20,000 Hz was measured by means of a TOA-111 spectrum analyzer, manufactured by the RFT company A single-filament data-unit with a sensing element consisting of gilded tungsten wire with a diameter of 5 μm and a length of 3 mm was used in the experiments. The data unit was moved by means of a coordinate mechanism with scale divisions of 0.01 mm. In measuring the boundary

A. N. Tupolev Kazan Aviation Institute. Translated from Inzhenerno-Fizicheskii Zhurnal, Vol. 48, No. 3, pp. 387-391, March, 1985. Original article submitted May 3, 1983.

 0022-0841/85/4803-0276$09.50

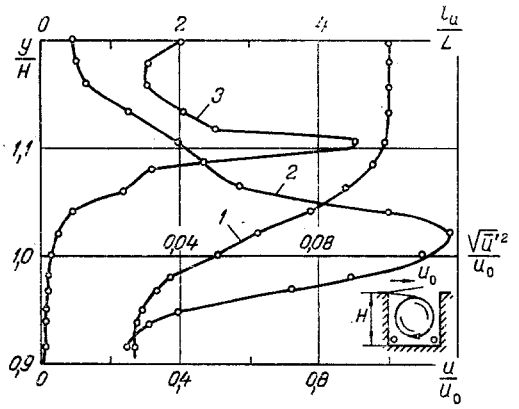

Fig. 1. Flow parameters in the mixing layer above the cavity for H/L = 1.0, x/L = 0.5. 1) u/u_0; 2) $\sqrt{\overline{u'^2}}/u_0$; 3) l_u/L.

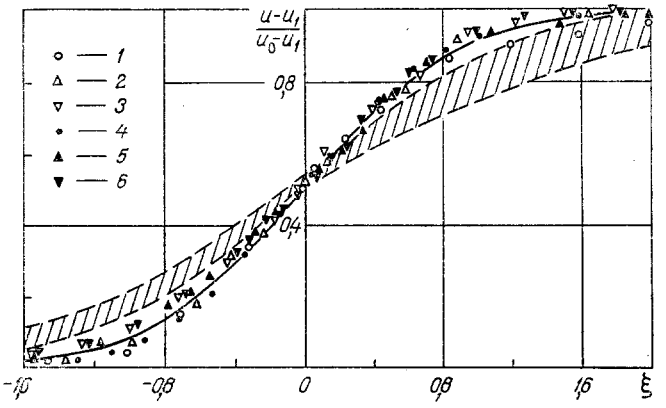

Fig. 2. Velocity profile in the mixing layer for H/L = 1.0: 1) x/L = 0.25; 2) 0.5; 3) 0.75; H/L = 0.5: 4) x/L = 0.25; 5) 0.5; 6) 0.75. $\xi = \sigma y/x$.

layer characteristics near a wall, a KM-8 cathetometer was used for coordinating the data unit with an accuracy to 0.005 mm.

A characteristic feature of the mixing layer developing from the flow separation point above the cavity is its interaction with the circulation flow inside the cavity, whose velocity along the mixing layer first increases to a maximum and then decreases to zero in approaching the attachment point. Figure 1 shows the profiles of the mean velocity, the rms values of turbulent fluctuations, and the integral turbulence scale in the mixing layer above the central section of the cavity. The mean velocity at the lower boundary of the mixing layer reaches a value equal to 0.25-0.30 of the outer flow velocity. The turbulent fluctuation maximum is shifted toward the outer flow; its value is approximately equal to $0.12u_0$. The profile of the integral turbulence scale is essentially nonuniform and has a characteristic maximum at the outer boundary of the mixing layer. According to our measurements, the integral turbulence scale within the cavity has values amounting to 0.05-0.1L.

Similar measurements were also performed in other sections of the mixing layer. They have shown that the turbulence intensity along the mixing layer increases somewhat, while the layer thickness increases according to roughly the same law as in the ordinary mixing layer of free associated flows [4]. The mean expansion coefficient of the mixing layer along the cavity is equal to $k = d\delta/dx \approx 0.24$. Our measurements show that the velocity profile for cavities with H/L = 1.0 and 0.5 varies slightly along the mixing layer and is virtually self-similar (Fig. 2). It is in good agreement with Görtler's theoretical relationship [5] (solid curve) if the effect of the initial boundary layer ahead of the separation point on mixing layer

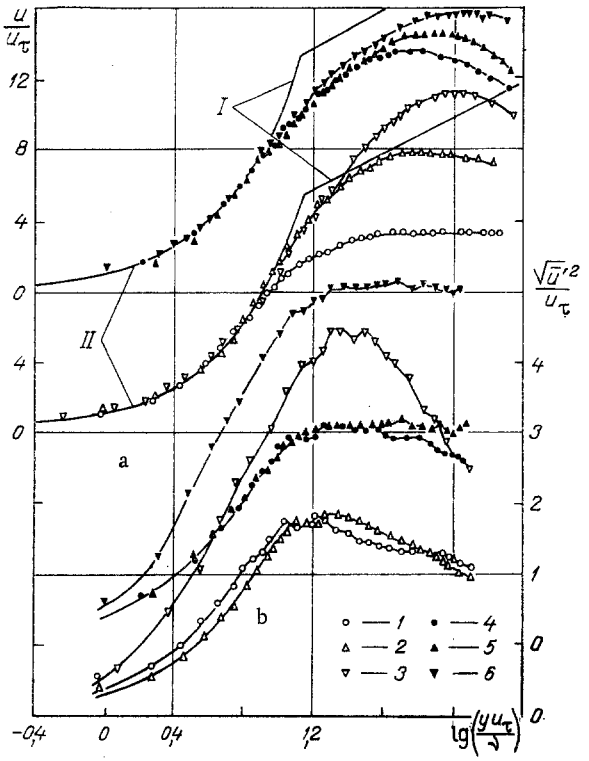

Fig. 3. Velocity (a) and turbulent fluctuation (b) profiles in the boundary layer at the cavity bottom for H/L = 1.0: 1) x/L = 0.25; 2) 0.5; 3) 0.75 and H/L = 0.5: 4) x/L = 0.25; 5) 0.5; 6) 0.75; I) $u/u_\tau = 5.8 - 2.61\ln\frac{yu_\tau}{\nu}$; II) $-\frac{u}{u_\tau} = \frac{yu_\tau}{\nu}$.

development is taken into account by means of Kirk's method [6]. According to this method, the effect of the boundary layer can be accounted for approximately by shifting the effective origin of the mixing layer upstream from the separation point by a length equal to 30 momentum loss thicknesses in the oncoming boundary layer. For comparison, this figure also shows the experimental data (hatched area) for the case where the separation point was used as the initial point of mixing layer development.

Our experiments have shown that the boundary layer at the cavity bottom develops under conditions of accelerated — retarded flow with high turbulence and is characterized by small values of the Reynolds number. Under our experimental conditions, the Reynolds numbers calculated with respect to the momentum loss thickness δ^{**} and the velocity at the outer limit of the boundary layer at the cavity bottom u_δ were equal to $Re^{**} = 40\text{-}180$. Experiments have shown that the investigated boundary layer is characterized by a number of specific features. In the first place, we note the thick, viscous sublayer with a thickness of $0.1\text{-}0.15\delta$ and the high degree of turbulence in the outer part of the boundary layer, which reaches values of $\sqrt{u'^2}/u_\delta = 0.2\text{-}0.3$.

Figure 3a shows the experimental velocity profiles for the boundary layer at different sections along the cavity bottom, with the exception of the regions near the corners ($x/L \leqslant 0.1$ and $x/L \geqslant 0.9$), where secondary vortices were developing. For the sake of comparison, this figure also shows the velocity profile — the linear ($u/u_\tau = yu_\tau/\nu$) and the logarithmic ($u/u_\tau = A + 1/\varkappa \ln yu_\tau/\nu$) segments — in an ordinary boundary layer on a plate. The coefficients $A = 5.8$ and $\varkappa = 0.385$ in the logarithmic relationship correspond to the boundary layer at the wall ahead of the separation point of the outer flow. In the immediate vicinity of the wall, the experimental data are in satisfactory agreement with the linear segment of the velocity profile. As for the outer part of the investigated boundary layer, it is evident that it is not described by a logarithmic relationship in any of the flow regions: the accelerated ($x/L \leqslant 0.4$), the gradient-free, and the retarded ($x/L \geqslant 0.6$) flow regions.

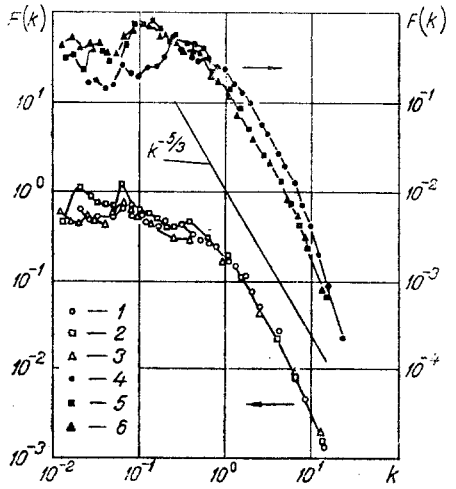

Fig. 4. Energy spectra of turbulent velocity fluctuations in the central section at the cavity bottom for H/L = 1.0: 1) y/δ = 0.14; 2) 0.75; 3) 1.5 and H/L = 0.5: 4) y/δ = 0.11; 5) 0.75; 6) 1.5; F(k), cm; k, cm^{-1}.

In connection with this, it should be noted that, in numerical simulation of flow in a cavity and other detached flows, the boundary layer, as a rule, is approximated by a single logarithmic relationship of the type $\frac{u}{u_\tau} = A + \frac{1}{\varkappa} \ln \frac{yu_\tau}{\nu}$ [7-9]. The distribution of turbulent fluctuations over the cavity bottom for the investigated range of H/L values has qualitatively the same character (Fig. 3b). The level of turbulent fluctuations increases considerably in the retarded flow region $(x/L \geqslant 0.6)$.

Figure 4 shows the normalized spectra of longitudinal velocity fluctuations with respect to wave numbers F(k), measured in the central section of the boundary-layer flow at the cavity bottom. The spectra were measured at three points: within the viscous sublayer, in the outer region, and beyond the confines of the boundary layer. One notices the presence of an equilibrium subregion in the wave number range k = 1-10 cm^{-1}, which is common to all spectra. Considerable nonuniformity in the normalized spectrum distribution with respect to wave numbers F(k) is observed in the range of small wave numbers.

NOTATION

x, y, Cartesian coordinates; H and L, depth and length of the cavity, respectively; u, mean velocity component; $\sqrt{\overline{u'^2}}$, rms value of the fluctuation component of velocity; δ, boundary layer thickness; δ**, momentum loss thickness; ν, kinematic viscosity; τ, friction stress; l_u, integral longitudinal turbulence scale; $u_\tau = \sqrt{\tau/\rho}$, friction velocity; $\xi = \sigma \frac{y}{x}$, dimensionless coordinate along the mixing layer thickness; σ = 13.5, experimental constant; $Re_L = u_0 L/\nu$, and $Re^{**} = u_\delta \delta^{**}/\nu$, Reynolds numbers. Subscripts: 0, outer flow parameters; 1, quantities at the mixing layer boundary on the cavity side; δ, quantities pertaining to the outer limit of the boundary layer at the wall.

LITERATURE CITED

1. A. V. Gorin, "Survey of calculation models for incompressible liquid flow in a square cavity," in: Gradient and Detached Flows [in Russian], Izd. Sib. Otd. Akad. Nauk SSSR, Novosibirsk (1976), pp. 85-116.
2. L. V. Gogish and G. Yu. Stepanov, "Turbulent detached flow," Izv. Akad. Nauk SSSR, Mekh. Zhidk. Gaza, No. 2, 31-47 (1982).
3. J. O. Hinze, Turbulence, McGraw-Hill (1960).
4. G. N. Abramovich, Applied Gas Dynamics [in Russian], Nauka, Moscow (1976).
5. H. Schlichting, Boundary Layer Theory, McGraw-Hill (1974).

6. K. E. Yurchenok, "Effect of the boundary layer at the separation point on the bottom pressure in supersonic gas flow," Transactions of the Leningrad Institute of Aircraft Instrument Construction (Tr. LIAP) [in Russian], Vol. 85, Leningrad (1974), pp. 88-99.
7. A. D. Gosman, E. E. Hallil, and J. G. Whitelaw, "Calculation of two-dimensional turbulent recirculation flow," in: Turbulent Shear Flow [Russian translation], Vol. 1, Mashinostroenie, Moscow (1982), pp. 247-269.
8. P. Bradshaw (ed.), Turbulence [Russian translation], Mashinostroenie, Moscow (1980).
9. Ya. I. Kabakov and A. I. Maiorova, "Turbulent flow in a rectangular cavity in the channel wall," Inzh.-Fiz. Zh., 46, No. 3, 363-371 (1984).

MEASUREMENT OF MOIST AIR VELOCITY BY MEANS OF HOT-WIRE ANEMOMETERS

I. L. Povkh, P. I. Savostenko, and Yu. D. Ukrainskii

UDC 533.601

The effect of air humidity on the accuracy of measurements by means of constant-temperature hot-wire anemometers is investigated, and a method for reducing the resulting error is described.

The hot-wire anemometer is presently one of the most widely used instruments for turbulent flow measurements. There is a large number of publications on the most diverse aspects of hot-wire anemometer use [1]. Papers on interpretation of hot-wire anemometer measurement results for a wide range of medium parameters, such as the pressure, the density, the temperature, etc. [2], are published regularly. Nevertheless, the effect of humidity on the accuracy in measuring the velocity characteristics of gaseous media by means of hot-wire anemometers has not received enough attention in the domestic literature.

We shall consider here a "constant-temperature (resistance)" hot-wire anemometer (CTHWA) [3, 4], which has lately been used widely in practice, especially for measurements in air [5, 6].

Neglecting the effect of the filament's thermal radiation, which is indeed proper for air at the usual operating temperatures in the 250-300°C range [1, 3], we write the semi-empirical Kramers expression for heat exchange under steady-state conditions [3] for the filament:

$$U^2 = \frac{R_w (R_w - R_g)}{bR_0} l\pi \left[K_f^{0.8} (c_p \mu_f)^{0.2} + 0.57 K_f^{0.67} (c_p \mu_f)^{0.33} (\rho_f dv/\mu_f)^{0.5}\right], \quad (1)$$

where b is the thermal coefficient of the filament resistivity if we assume that the temperature dependence of the resistance R_w is linear, i.e., $R_w \approx R_0[1 + b(\theta_w - \theta_0)]$, where R_0 is the filament's resistance at $\theta_0 = 273°K$.

It is evident that the values of K_f, μ_f, c_p, and ρ_f for air depend on the amount of water vapor in the air. Let us determine the form of these relationships and write, in the final analysis, expression (1) as a function of the humidity.

The expressions for K_f and μ_f are known from the kinetic theory of gases [7] (since our considerations pertain to virtually normal conditions, we shall henceforth consider air and the water vapor in it as an ideal gas):

Translated from Inzhenerno-Fizicheskii Zhurnal, Vol. 48, No. 3, pp. 392-396, March, 1985. Original article submitted December 26, 1983.

 0022-0841/85/4803-0280$09.50